Meandering of laminar channels

By **OLIVIER DEVAUCHELLE, CHRISTOPHE JOSSERAND PIERRE-YVES LAGRÉE and STÉPHANE ZALESKI**

Institut Jean le Rond d'Alembert, Université Pierre et Marie Curie - Paris 6, CNRS-UMR 7190, Case 162, 4 place Jussieu, 75252 Paris Cédex 05-France

(Received 8 February 2007)

A two dimensional model for the erosion generated by viscous free-surface flows, based on shallow-water equations and the lubrication approximation is presented. It has a family of self-similar solutions for straight erodible channels of invariant section, with an aspect ratio that increases in time. It is also shown, throught a simplified stability analysis, that a laminar river can generate meander-like and braid-like instabilities very similar to those observed in natural rivers. This supports the idea that meanders and braids do not require turbulence to develop. Finaly, we propose a simple interpretation for the transition between patterns observed in experimental erodible channels.

1. Introduction

Natural rivers seldom form straight beds. Instead, they usually develop braids or meanders as a consequence of current-induced sediment transport. The understanding of river sedimentation mechanisms can help to characterize the spatial heterogeneity of alluvial rocks, which is a key parameter when simulating aquifer flows or oil traps inpetroleum reservoirs (de Marsily *et al.* (2005)). The theoretical work of Reynolds (1965), Hansen (1967) and Callander (1969) introduced among geomorphologists the fruitful idea that such patterns may originate in the linear instability of the bed. Two-dimensional turbulent shallow water equations associated with a simple sediment transport law are able to predict the formation of alternate bars in channels of constant width, and it has been commonly accepted as a first approximation that such bars may generate braids and meanders (Parker (1976)). Numerous refinements of this theory may be found in the litterature: Engelund & Skovgaard (1973) performed the bar stability analysis in three dimensions, while Parker (1976) focused on the differentiation between braids and meanders. Later Ikeda *et al.* (1981) and Blondeaux & Seminara (1985) relaxed the rigid-banks hypothesis, and more recently Schielen *et al.* (1993) modelled the non-linear evolution of free bars. All these works (and to our knowledge, every study in this field) considered turbulent flows, which is entirely legitimate as far as natural rivers are concerned (the average Reynolds number of the Seine river in Paris is about 10^6). However, one should not conclude from this ubiquity of turbulence that braiding and meandering are inherently turbulent phenomena. Malverti *et al.* (2006) very recenlty accumulated experimental evidence showing that laminar flumes may generate all patterns created by real rivers. In particular, the constant flow of a thin liquid film down an homogeneous granular bed initially crossed by a straight channel exhibits rather complex pattern dynamics as the flume widens through erosion†. The present study investigate the theory of laminar rivers

† Personnal communication from E. Lajeunesse and F. Métivier

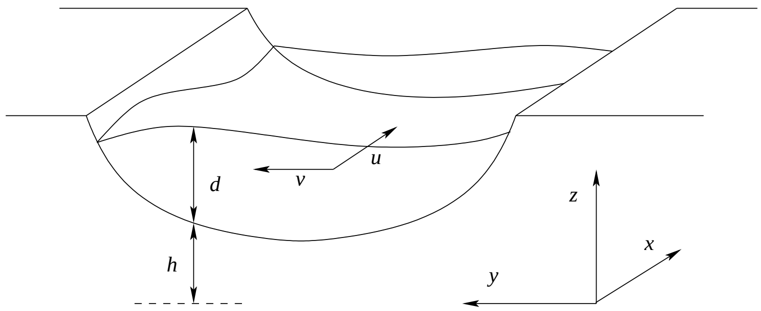

FIGURE 1. Sketch of a riverbed.

stability. Our objective is to support theoretically the idea that laminar flumes may be considered as models of their turbulent counterpart.

In a first section, a two-dimensional evolution model for laminar flumes is presented. It is mostly based on the assumption that the velocity profile is of Poiseuille's type, and that the shallow-water theory holds. The following sections are devoted to two simple, analytically tractable cases: the translation invariant straight river with erodible bed, and the linear stability of a channel of constant width.

2. A two-dimensional model

Let us consider an experiment during which an initial channel incised into a uniform and non-cohesive sand layer is eroded by a viscous flow. If the slope of the sand bed remains small enough, one may use two-dimensional equations to model both the water flow and the sediment transport. A rather general and commonly used assumption for morphogenesis consists in the time-scale separation between the flow and erosion process: the bed evolves slowly enough for the flow to be quasi-static(see Parker (1976), Callander (1969), Engelund & Skovgaard (1973) and Blondeaux & Seminara (1985)). In the present article the following notations are used (see also figure 1):

- x and y are the coordinates in the plane of the experiment, the first aiming toward the main slope. z is the coordinate normal to the plate;
- h is the elevation of the sand surface and d is the water depth ($h + d$ is thus the water level);
- $\mathbf{u} = (u, v)$ is the vertically averaged water velocity, the horizontal water flux components being ud and vd;
- S is the plate tilt;
- g is the magnitude of gravity, and ν is the kinematic viscosity of water.

2.1. *Water flow*

For sufficiently low values of the Reynolds number, one may consider that the flow is close to Poiseuille's one. The water velocity is thus represented by a parabolic velocity profile which adapts instanteanously to the topography (this corresponds to the lubrication approximation). Secondary currents are thus neglected, although many authors believe they strongly influence erosion in developped meanders (see for example Blankaert & de Vriend (2004)). For viscous flumes however, this is probably not an essential feature. The vertical integration of the Navier-Stokes equations leads to the viscous shallow water equations:

$$\frac{6}{5}(\mathbf{u} \cdot \nabla)\mathbf{u} = g\left(-\nabla(d+h) + S\mathbf{e}_x\right) - \frac{3\nu}{d^2}\mathbf{u}, \tag{2.1}$$

$$\nabla \cdot (\mathbf{u}d) = 0, \tag{2.2}$$

where $\mathbf{e}_x$ is the unit vector parallel to the x-axis. These equations are very similar to those used for turbulent rivers, except for the friction terms (proportional to $|\mathbf{u}|/d^2$ in the present case, and to $|\mathbf{u}|^2/d$ in the turbulent case).

2.2. *Sediment transport*

The river bed evolves under the influence of both erosion and avalanches. In the present context erosion consists of flow-induced entrainement of sand grains. On the other hand, avalanches are collective phenomena triggered by an excess slope of the sand surface. The continuous model here developped can only handle the average effects of erosion and avalanches. This approximation allows for the definition of a total sediment flux $\mathbf{q}(x, y, t)$ integrated along the vertical direction. Considering the strong time scale separation between erosion and avalanches, one may assume that the associated flux (respectively $\mathbf{q}_e$ and $\mathbf{q}_a$) are independant. The continuity equation for sand then reads:

$$\frac{\partial h}{\partial t} = -\nabla \cdot \mathbf{q}, \tag{2.3}$$

where $\mathbf{q} = \mathbf{q}_e + \mathbf{q}_a$. Closure relations derived on dimensional and empirical grounds link (2.3) to the flow equations. Most of the relations between the sediment flux and the flow are proposed in the litterature as functions of the Shields number θ, which expresses the ratio between hydrodynamic forces exerted on a grain to its apparent weight :

$$\theta = \frac{|\tau|}{(2r)(\rho_g - \rho_w)g}, \tag{2.4}$$

where r, ρ_w, ρ_g and τ are respectively the typical particule radius, the density of water, the density of a grain and the bottom shear stress. We follow Balmforth & Pronvenzale (2001) who propose the following expression as a classical relationship for small slope:

$$\mathbf{q}_e = \phi(\theta)\left(\frac{\tau}{|\tau|} - \mathbf{G}\cdot\nabla h\right), \tag{2.5}$$

where ϕ is a growing function that may include a threshold value, and $\mathbf{G}$ is a diagonal operator. On the basis of his experiments in the viscous flow regime, Charru *et al.* (2004) suggests that $\phi(\theta) \propto \theta(\theta - \theta_c)$ above the threshold value θ_c. Such a threshold may control the shape of equilibrium river bed (see section 3). However, this threshold is hardly distinguished experimentally from a continuous decay of ϕ. A simpler relation such as $\phi(\theta) = \phi_0\theta^\beta$ (where ϕ_0 and β are empirical constants) may fit satisfactorily the same data (for instance with $\beta = 5$ which is the value used by Schielen *et al.* (1993)). The second term in (2.5) reproduces the slope-induced deviation of the sediment flux. Schielen *et al.* (1993) set $\mathbf{G} = \gamma\mathbf{I}$ where γ is a constant of order one. This term is essential to cut-off short wavelength instabilities (see Section 4.2). In the frame of the laminar Saint-Venant approximation, the above sediment transport equation becomes

$$\mathbf{q}_e = E_e\left(\frac{|\mathbf{u}|}{d}\right)^\beta\left(\frac{\mathbf{u}}{|\mathbf{u}|} - \gamma\nabla h\right), \tag{2.6}$$

with $E_e = \phi_0(3\rho_w\nu/((2r)(\rho_g - \rho_w)g))^\beta$.

The full dynamics of avalanches is far out of the scope of this study. Instead, we may propose a simple model which reproduce the following features:

- the sand mass is conserved through the avalanche process;
- there are no avalanches under a critical slope α;
- above the critical angle, $\mathbf{q}_a$ is directed toward the main slope and increases with the slope value.

Considering these criteria, we propose the following expression :

$$\mathbf{q}_a = -E_a \mathcal{F}\left(|\nabla h|\right) \frac{\nabla h}{|\nabla h|}, \tag{2.7}$$

where $\mathcal{F}(\cdot) = (\cdot - \alpha)\mathcal{H}(\cdot - \alpha)$, $\mathcal{H}$ stands for the Heavyside function and E_a is a constant.

2.3. *Boundary conditions*

Flow equations (2.1) and (2.2) together with sediment transport equations (2.3), (2.6) and (2.7) form a closed system. To solve this system in the fixed domain Ω, conditions must be specified on its boundary $\partial\Omega$. Their general form is

$$\lambda_u d + \mu_u \mathbf{u} \cdot \mathbf{n} = \pi_u, \ \lambda_h h + \mu_h \mathbf{q} \cdot \mathbf{n} = \pi_h, \tag{2.8}$$

where λ_u, μ_u, π_u, λ_h, μ_h and π_h are functions to be specified. $\mathbf{n}$ is the unit vector normal to $\partial\Omega$, aiming outward. In the general case, Ω may include sub-domains where $\mathbf{q} = 0$. In such domains, the evolution equation becomes $\partial h/\partial t = 0$.

If one wants to restrict the analysis to the active sub-domain $\Omega_+(t)$ where $\mathbf{q} \neq 0$, the conditions to be imposed on its mobile boundary $\partial\Omega_+(t)$ are

$$\mathbf{u} \cdot \mathbf{n} = 0, \ \mathbf{q} \cdot \mathbf{n} = c(h_+ - h_-), \frac{\mathrm{d}h_+}{\mathrm{d}t} = -\nabla \cdot \mathbf{q}_+ + c\left(\mathbf{n} \cdot \nabla h_+ + \mathbf{n} \cdot \nabla h_-\right). \tag{2.9}$$

In the above equations, c is the normal velocity of the $\partial\Omega_+(t)$, the subscripts a and b denotes quantities evaluated respectively inside and outside $\Omega_+(t)$. $\mathrm{d}/\mathrm{d}t$ is the convective derivative at a point of $\partial\Omega_+(t)$ moving with velocity $c\mathbf{n}$. The first boundary condition reflects the time scale separation between flow and erosion. The following ones correspond to the sediment mass conservation equations integrated over a small domain crossed by $\partial\Omega_+(t)$. A special case of these boundary conditions has been derivated by Kovacs & Parker (1994). The classical conditions for non-erodible and impermeable banks are obtained by setting $c = 0$.

3. Prismatic channels

For a straight (that is, x-invariant) river, the equations derived in section 2 become a one dimensional non-linear diffusion equation which admits self-similar solutions. The reader interested in the problem of realistic river cross-section, a complex two-dimensionnal problem in the general case, may refer to Parker (1978*a*), Parker (1978*b*), Kovacs & Parker (1994), Paquier & Khodashenas (2002) and Stark (2006) among others.

3.1. *A non-linear diffusion equation*

Any quantity may only depend on time and the transverse coordinate: $h = H(y,t)$, $d = D(y,t)$, $u = U(y,t)$ and $v = V(y,t)$. The flow equations (2.1) and (2.2) thus give

$$U = \frac{gS}{3\nu} D^2, \ V = 0, \ D + H = \eta(t). \tag{3.1}$$

In the last equation, the water level η is a function of time only. The water discharge $Q_w = \int_{-\infty}^{\infty} UD\mathrm{d}y$ is usually controlled in laboratory experiments, which governs the evolution of $\eta(t)$. For the sake of simplicity, we will consider in what follows that η is a constant (this case represents a river supplied by an infinite reservoir; this arbitrary constant is set to zero). In that case the sediment transport equations (2.3), (2.6) and (2.7) lead to

$$\frac{\partial D_*}{\partial t_*} = \gamma \frac{\partial}{\partial y_*}\left(D_*^{\beta}\frac{\partial D_*}{\partial y_*}\right) - \frac{1}{\epsilon_a}\frac{\partial}{\partial y_*}\left(F\left(\left|\frac{\partial D_*}{\partial y_*}\right|\right)\operatorname{sign}\left(\frac{\partial D_*}{\partial y_*}\right)\right). \tag{3.2}$$

In the above equation, the starred quantities are dimensionless. The initial width W and depth D_0 of the river are respectively horizontal and vertical characteristic lengths. $T = (3\nu/(gS))^{\beta}/(E_e D_0^{\beta-2})$ is the typical widening timescale. $\epsilon_a = E_a/(TD_0^2)$ is a non-dimensional number which compares typical avalanches flux to erosion ones, and may be considered very small.

3.2. *Self-similar solutions*

If the transverse slope of the channel $\partial H/\partial y$ remains smaller than the critical slope α, no avalanche occurs. This particular case has simple self-similar solutions of the form

$$D_*(y_*, t_*) = \frac{1}{t_*^{1/(\beta+2)}} f(\chi). \tag{3.3}$$

where $\chi = \frac{y_*}{t^{1/(\beta+2)}}$. (3.2) leads to

$$\frac{\partial}{\partial \chi}\left(\gamma f^{\beta}\frac{\partial f}{\partial \chi} + \frac{\chi f}{\beta+2}\right) = 0. \tag{3.4}$$

If f_s is a simmetrical solution to (3.4) (that is, if $\mathrm{d}f_s/\mathrm{d}\chi = 0$ at $\chi = 0$), then integration of (3.4) gives

$$f_s(\chi) = \left(A - \frac{\beta}{2\gamma(\beta+2)}\chi^2\right)^{1/\beta}, \tag{3.5}$$

where A is a constant. Only for $\beta = 1$ does $D_{*,s}$ behave regularly at the banks. In that case, the river cross-section is a parabola. It width increases as $t^{1/3}$ while it shallows as $t^{-1/3}$. This widening corresponds to the behaviour of laboratory rivers (for example in the experiments of Nakagawa (1983) and Federici & Paola (2003)) . If the initial shape is flat enough to avoid avalanches, this condition holds at any time. Unfortunately this case cannot model erosion patterns formation, for it is uncondionally stable (see section 4).

On the other hand, if $\beta > 1$ (this is usually the case, see section 2.2), the picture is quite different. The continuous widening process still holds (although with different power laws), but the bed slope $\mathrm{d}D_{*,s}/\mathrm{d}y_*$ diverges at the banks. Thus avalanches must occur at the banks, and the self-similar solution fails. This behaviour is observed in laboratory experiments (see Nakagawa (1983) among others), and was already pointed out by Kovacs & Parker (1994). The effect of bank avalanches is uneasy to quantify analyticaly. According to numerical simulations however (see figure 2), they do not seem to influence strongly the bed evolution far enough from the banks. Consequently one may still use the results of the self-similar theory as good approximations of true solutions.

4. Linear stability

Experimental channels such as the one of Federici & Paola (2003) often remain stable for a while, then develop meanders which in turn are followed by more complex braided-

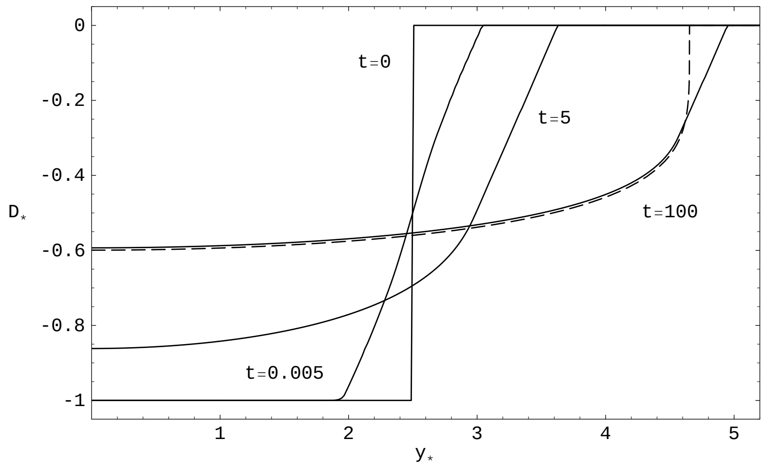

FIGURE 2. Widening of a straight laminar channel through erosion, modelled with (3.2). Parameter values are $\epsilon_a = 0.1$, $\alpha = 0.8$ and $\gamma = 1$. Solid lines: numerical solutions of (3.2) at different times. Dashed line: self-similar solution (without avalanches, see section 3.5) at $t = 100$. The presence of avalanches (solid lines) seems not to influence much the evolution of the profile.

like patterns. This scenario of transitions (sometimes called *ageing*) may be interpreted as the successive dominance of different unstable modes. If the widening process presented in the previous section is slow enough, D_{s*} may be choosen as a quasi static base state for a stability analysis. In what follows, we will disregard any interaction between widening and instabilities.

4.1. *Derivation of the dispersion relation*

In order to present the simplest stability model which keeps the essential features of channel stability, we will consider a rectangular base state with solid-wall boundaries, of width W and depth D_0 (its aspect ratio is thus $R = W/D_0$). The boundary conditions at the bank are $\mathbf{u}\cdot\mathbf{n} = 0$ and $\mathbf{q}\cdot\mathbf{n} = 0$. The water velocity is uniform and parallel to the x-axis ($U_0 = gSD_0^2/(3\nu)$), and so is the basic sediment flux ($Q_0 = E_e(U_0/D_0)^\beta$). Let us seek travelling-wave perturbations of this base state:

$$\varphi(x,y,t) = \varphi_0 + \epsilon\varphi_*\left(\frac{y}{W}\right)e^{i(kx/W-\omega t/(TR))}, \tag{4.1}$$

where $\varphi = (u, v, h, d, q_x, q_y)$. The base state corresponds to $\varphi_0 = (U_0, 0, -D_0, D_0, Q_0, 0)$ and the perturbation is $\varphi = (U_0u_*, U_0v_*, D_0h_*, D_0d_*, Q_0q_{x,*}, Q_0q_{y,*})$. $T = D_0W/(RQ_0)$ is a characteristic time for erosion (see section 3.1) and ϵ is a small dimensionless amplitude of the perturbation. k is a real dimensionless wavenumber whereas ω is complex in the general case. (2.1), (2.2), (2.6) and (2.3) lead to the following system:

$$\left(\frac{6}{5}F^2ik + RS\right)u_* + ikh_* + (ik - 2RS)d_* = 0, \tag{4.2}$$

$$\left(\frac{6}{5}F^2ik + RS\right)v_* + \frac{\mathrm{d}d_*}{\mathrm{d}y} + \frac{\mathrm{d}h_*}{\mathrm{d}y} = 0,\ ik(d_* + u_*) + \frac{\mathrm{d}v_*}{\mathrm{d}y} = 0, \tag{4.3}$$

$$-i\omega h_* + ikq_{x,*} + \frac{\mathrm{d}q_{y,*}}{\mathrm{d}y} = 0,\ q_{x*} = \beta u_* - \frac{ik\gamma}{R}h_* - \beta d_*,\ q_{y*} = v - \frac{\gamma}{R}\frac{\mathrm{d}h_*}{\mathrm{d}y}. \tag{4.4}$$

In the above sytem, $F = U_0/(gD_0)^{1/2}$ is the Froude number of the unperturbed channel. This system may be reduced to

$$\frac{\mathrm{d}^4 h_*}{\mathrm{d}y^4} + A\frac{\mathrm{d}^2 h_*}{\mathrm{d}y^2} + Bh = 0, \quad \frac{\mathrm{d}^3 h_*}{\mathrm{d}y^3}\left(\frac{1}{2}\right) = \frac{\mathrm{d}h_*}{\mathrm{d}y}\left(\frac{1}{2}\right) = \frac{\mathrm{d}^3 h_*}{\mathrm{d}y^3}\left(-\frac{1}{2}\right) = \frac{\mathrm{d}h_*}{\mathrm{d}y}\left(-\frac{1}{2}\right) = 0. \tag{4.5}$$

In the above equation,

$$A = \big(36F^4k^3\gamma + 30F^2k\big(-2k^2\gamma - ikR(1+\beta+4S\gamma) + iR\omega\big) + 25RS\big(2ik^2\gamma + kR(-3+\beta-3S\gamma) + R\omega\big)\big)/\big(5\big(6F^2k - 5iRS\big)\gamma\big), \tag{4.6}$$

$$B = \frac{1}{\gamma}\left(k\left(k^3\left(\gamma - \frac{6F^2\gamma}{5}\right) + ik^2R(2\beta + 3S\gamma) + \frac{1}{5}i\big(-5+6F^2\big)kR\omega + 3R^2S\omega\right)\right). \tag{4.7}$$

Let s be a solution of the characteristic equation attached to (4.5). Applying the boundary conditions leads to $s = in\pi$, where n is an integer. Finally, one may derive the dispersion relation from (4.5) :

$$\omega = \big(5kR\big(5iRS\big(-n^2\pi^2(-3+\beta) + 2k^2\beta\big) - 6F^2k\big(2k^2\beta + n^2\pi^2(1+\beta)\big)\big) - i\big(k^2+n^2\pi^2\big)\big(6F^2k - 5iRS\big)\big(\big(-5+6F^2\big)k^2 - 5n^2\pi^2 - 15ikRS\big)\gamma\big)/ \big(R\big(6F^2k - 5iRS\big)\big(\big(-5+6F^2\big)k^2 - 5n^2\pi^2 - 15ikRS\big)\big). \tag{4.8}$$

4.2. *Results interpretation*

The linear stability of a channel depends on the sign of the maximum growth rate over n and k, respectively the transverse and longitudinal wavenumbers. We will thus focus on the imaginary part σ of ω in what follows. Let σ_m be the maximum growth rate, and k_m and n_m the corresponding wavenumbers (*i.e.* $\sigma_m = \sigma(k_m, n_m) = \max_{k\in\mathbb{R},n\in\mathbb{N}}(\sigma)$). The transverse wavenumber n characterizes the instability pattern: $n = 0$ for y-invariant dunes (this mode can also initiate step-pool instability), $n = 1$ for meanders and $n > 1$ for braided patterns. The present theoretical frame fails to predict the step-pool instability often observed in narrow channels (Giménez (2003)), as σ is always negative for $n = 0$. This is not surprising for the phase-shift between the bed deformation and the water shear stress is neglected here (this phase shift controls sand ripple formation, see Kouakou & Lagrée (2006)). The fluid and sediment choices determine parameters γ and β. Both parameters are crucial to the present model, although a change in numerical values does not lead to a major qualitative change in the results. The diffusion term which is proportional to γ stabilizes the high n modes. Without it, the higher n, the higher σ_m. As in Schielen *et al.* (1993), we take $\gamma = 1$ in the following. If $\beta = 1$, that is if the sediment flux is proportional to the shear stress, then no instability ever appears (again σ is always negative in that case). Instability may occur only if $\beta > 1$. $\beta = 5$ is choosen hereinafter as an illustrative case (see section 2.2).

Figure 3 illustrates the transition to bed instability as the aspect ratio is increased, for constant tilt and Froude number. A deep and narrow ($R = 8$) channel is stable, as for no values of n and k can σ be negative. A shift to $R = 20$ allows for the $n = 1$ mode

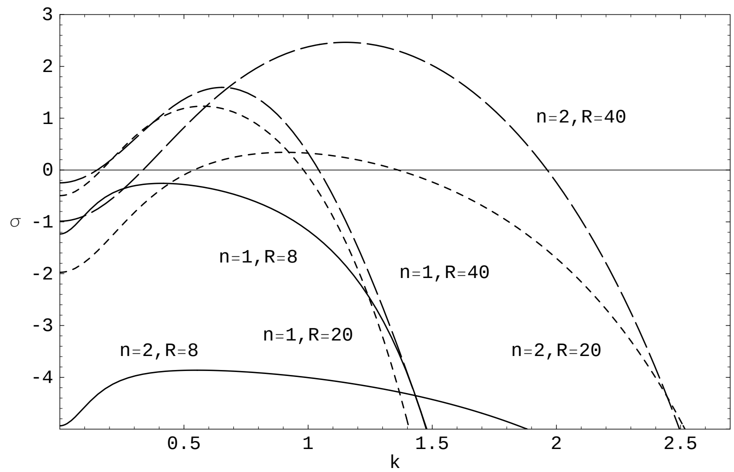

FIGURE 3. Linear growth rate σ of bed instability in a laminar river, versus the corresponding non-dimensional wave number k. The parameters values are $F = 1.5$, $\beta = 5$, $\gamma = 1$, $S = 0.0524$. For each value of the aspect ratio, both the modes n =1 and 2 are represented. Solid curves: $R = 8$; short dashes: $R = 20$; long dashes: $R = 40$. As the aspect ratio is increased, the most instable mode switches from $n = 1$ to $n = 2$. This behaviour provides an interpretation for the transition in patterns observed in some experiments.

to be unstable. For a still wider channel ($R = 40$), both $n = 1$ and $n = 2$ modes are unstable, but the latter grows faster. These transitions can be summarized in a three-dimensional phase diagram, with coordinates R, F and S. A constant S slice of this diagram is presented in figure 4. Such a diagram provides a crude interpretation for the ageing of laminar laboratory rivers. Let us consider for example the case of section 3, for which the mean water level is fixed, while its bed and banks are freely eroded. The tilt S remains constant troughout the experiment whereas, in accordance with (3.5), the Froude number and aspect ratio evolve as follows:

$$R \propto t^{2/(\beta+2)}, \; Fr \propto t^{3/(2(\beta+2))}. \tag{4.9}$$

This parameterized curve correspond to $F = F_0(R/R_0)^{3/4}$ in the stability diagram (the subscript 0 denotes initial conditions). In most cases this curve comes successively through the three stability domains of figure 4. If the water output is conserved instead of the water level (this conditon is more common in experiments), the straight channel evolution is characterized by $F = F_0(R/R_0)^{-3/8}$. Again, for realistic initial conditions (typically $R_0 = 5$, $F = 1.5$), the river undergoes different instability regimes as it ages. If a threshold is introduced in the erosion law, the river eventually reaches an equilibrium state. The position of this equilibrium in the stability diagram is an indication about the instability patterns the river will preferentially develop. For instance, we may expect that a river will develop meanders if its equilibrium state lies in the domain where the $n = 1$ mode is the most instable one.

5. Conclusion

The present paper demonstrate that viscous flows are able to generate braids and meanders, as turbulent rivers do. This statement, first suggested by Malverti *et al.* (2006), supports experimental stability studies on small-scale rivers. Also, it discharges models with the complexity of turbulence models. This may facilitate the examination of some

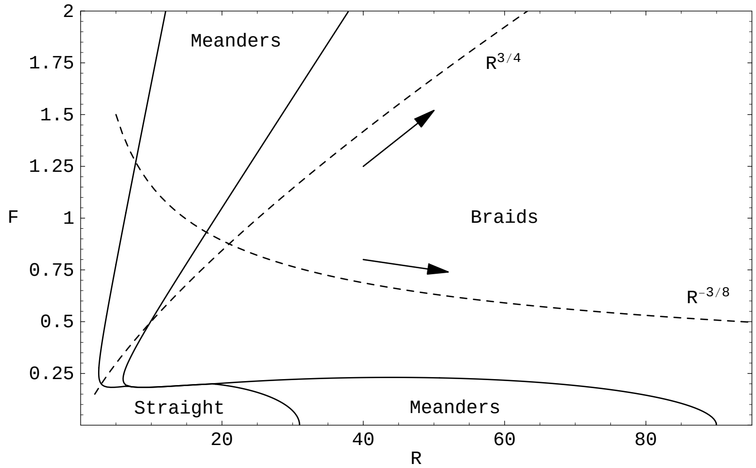

FIGURE 4. Stability diagram for a laminar channel. The domains (separated by solid lines) are named after the most instable mode n_m. "Straight": no instable mode; "Meanders": $n_m = 1$; "Braids": $n_m > 1$. The parameters values are $\beta = 5$, $\gamma = 1$ and $S = 0.0524$. The dashed lines represent the evolution of a straight river when the water level is imposed ($F = F_0(R/R_0)^{3/4}$) or when the outflow is imposed ($F = F_0(R/R_0)^{-3/8}$).

remaining difficulties of the problem, such as non-linearities or bank evolution. Hence in a first attempt to develop viscous channel stabilty models, we presented a two dimensionnal shallow-water model. A very simplified analytical approach based on this model was sufficient to describe qualitatively the ageing process observed in some experiments. A diagram presenting the dominant unsable modes with respect to the channel tilt, Froude number and aspect ratio was obtained (figure 4), which shows a large domain of existence for the meandering mode ($n = 1$) at small Froude number. This suggests that developped meanders might be obtained experimentally when reducing the Froude number without changing the tilt and aspect ratio (for instance by using liquids more viscous than water).

It is our pleasure to thank B. Andreotti, P. Claudin, A. Fourrière, E. Lajeunesse, D. Lhuillier, L. Malverti, F. Métivier and G. Parker for inspiring and stimulating discussions.

REFERENCES

BALMFORTH, N. J. & PRONVENZALE, A., ed. 2001 *Geomorphological Fluid Mechanics*, chap. 16, pp. 394–402. Springer.

BLANKAERT, K. & DE VRIEND, H. 2004 Secondary flow in sharp open-channel bends. *J. Fluid Mech.* **498**, 353–380.

BLONDEAUX, P. & SEMINARA, G. 1985 A unified bar-bend theory of river meanders. *J. Fluid Mech.* **157**, 449–470.

CALLANDER, R. A. 1969 Instability and river channels. *J. Fluid Mech.* **36** (3), 465–480.

CHARRU, F., MOUILLERON, H. & EIFF, O. 2004 Erosion and deposition of particles on a bed sheared by a viscous flow. *J. Fluid Mech.* **519**, 55–80.

ENGELUND, F. & SKOVGAARD, O. 1973 On the origin of meandering and braiding in alluvial streams. *J. Fluid Mech.* **57** (2), 289–302.

FEDERICI, B. & PAOLA, C. 2003 Dynamics of channel bifurcations in noncohesive sediments. *Water Resour. Res.* **39** (6), 1162.

GIMÉNEZ, R. 2003 The interaction between rill hydraulics, rill geometry and sediment detachment: an experimental approach. PhD thesis, Katholieke Universiteit Leuven.

HANSEN, E. 1967 The formation of meanders as a stability problem. Basic Research Report 13. Copenhagen Technical University of Danemark.

Ikeda, S., Parker, G. & Saway, K. 1981 Bend theory of river meanders. part 1. linear development. *J. Fluid Mech.* **112**, 363–377.

Kouakou, K. K. J. & Lagrée, P.-Y. 2006 Evolution of a model dune in a shear flow. *European journal of Mechanics B-Fluids* **25** (3), 348–359.

Kovacs, A. & Parker, G. 1994 A new vectorial bedload formulation and its application to the time evolution of straight river channels. *J. Fluid Mech.* **267**, 153–183.

Lemieux, P.-A. & Durian, D. 2000 From avalanches to fluid flow: A continuous picture of grain dynamics down a heap. *Physical Review Letters* **85** (20), 4273–4276.

Malverti, L., Parker, G., Armstrong, L., Lancien, P., Lajeunesse, E., Métivier, F., Coleman, S., Smith, C. E., Davies, T. & Cantelli, A. 2006 Fluvial and subaqueous morphodynamics of laminar flow. *Sedimentology* (to appear).

de Marsily, G., Delay, F., J., G., Renard, P., Teles, V. & Violette, S. 2005 Dealing with spatial heterogeneity. *Hydrogeol. J.* **13**, 161–183.

Nakagawa, T. 1983 Boundary effects on stream meandering and river morphology. *Sedimentology* **30**, 117–127.

Paquier, A. & Khodashenas, S. 2002 River bed deformation calculated from boundary shear stress. *Journal of Hydraulic Research* **40** (5).

Parker, G. 1976 On the cause and characteristic scales of meandering and braiding in rivers. *J. Fluid Mech.* **76** (3), 457–480.

Parker, G. 1978*a* Self-formed straight rivers with equilibrium banks and mobile bed. part 1. the sand-silt river. *J. Fluid Mech.* **89**, 109–125.

Parker, G. 1978*b* Self-formed straight rivers with equilibrium banks and mobile bed. part 2. the gravel river. *J. Fluid Mech.* **89**, 127–146.

Reynolds, A. 1965 Waves on the erodible bed of an open channel. *J. Fluid Mech.* **22**, 113–133.

Schielen, R., Doelman, A. & de Swart, H. 1993 On the nonlinear dynamics of free bars in straight channels. *J. Fluid Mech.* **252**, 325–356.

Stark, C. 2006 A self-regulating model of bedrock river channel geometry. *Geophysical Research Letters* **33** (4).